

## Indices

- $a$  is the nozzle cut;  
 $0$  is the stagnation parameter; other letter indices denote characteristic points of the jet.

The linear dimensions are normalized to the nozzle radius at the exit.

## LITERATURE CITED

1. I. P. Ginzburg, *Aerohydrodynamics* [in Russian], Vysshaya Shkola, Moscow (1966).
2. B. G. Semiletenko and V. N. Uskov, "Empirical functions determining the location of shock waves in a jet flowing onto an obstacle perpendicular to its axis," *Inzh. -Fiz. Zh.*, **23**, No. 3 (1972).

## WAVE STRUCTURE OF A SUPERSONIC JET DISCHARGING INTO AN OPPOSING SUPERSONIC STREAM

E. I. Sokolov and V. N. Uskov

UDC 532.525.2:533.6.011.72

A similarity parameter is suggested for the longitudinal dimensions of the wave structure of a supersonic underexpanded jet discharging into an opposing supersonic stream, and empirical equations are obtained for the calculation of these dimensions.

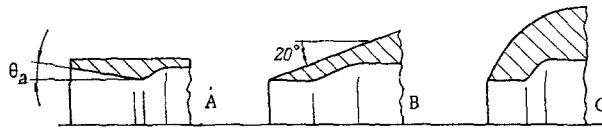
A number of reports devoted to the experimental investigation of the discharge of a supersonic jet into an opposing supersonic stream are presently known [1-6]. These investigations made it possible to establish the existence of two types of axisymmetric interaction of a jet with an opposing stream. If the underexpanded jet is retarded within the limits of the first barrel then an interface 1 concave to the jet (departing to infinity) and a disconnected bow shock wave 2 (type I flow) develop in the stream. Ahead of the surface, which is an impermeable barrier to the jet, a middle compression about 3 forms in the latter (Fig. 1). Near the bow surface of the body a circulation zone, closed or open depending on  $P = p_{0a}/p_{T\infty}$  and  $D = d_m/d_a$  develops with a pressure  $p_c$  different from  $p_\infty$  [2]. In flow of type II (penetration mode), observed with  $n \sim 1$ , the retardation of the jet occurs far ahead of the body, in its main section. The interaction of the jet and the stream has a nonsteady character. These types of flow are also observed in a rarefied stream [5, 6].

The wave structure formed in type I flow is analyzed below. A universal parameter of geometrical similarity of the longitudinal dimensions of the developing wave structure is suggested on the basis of the results of [1-4] and the experimental data of the authors. The presence of an infinite concave interface makes type I flow qualitatively similar to the well-studied flow when an underexpanded jet escaping into a flooded space with a pressure  $p_f$  acts on an infinite plane barrier. It is known [7] that in the case of the interaction with a barrier the introduction of the parameter  $N = M_a \sqrt{kn}$  makes it possible, by using the distance  $h$  to the barrier as the characteristic dimension, to obtain an empirical dependence connecting the standoff of the middle shock formed in the jet ahead of the barrier with its location and with the discharge parameters. On the basis of the indicated qualitative analogy of the processes, we apply the complex  $N$  to the analysis of experimental data on the location of the shock waves and the interface in the discharge of a jet into an opposing stream. The range of the parameters under consideration is given in Table 1. The distance  $x_m$  to the middle shock is used as the characteristic geometrical dimension in the investigated flow. This distance is calculated from the condition of equality of the stagnation pressures on the sides of the jet and the stream at the common critical point R (Fig. 1). When the distribution of Mach numbers  $M$  along the axis of the free jet is known this condition leads to the following equations for the determination of  $x_m$ :

$$\frac{p_{0a}}{p_{s\infty}} = \left( \frac{2}{k+1} M_m^{-2} + \frac{k-1}{k+1} \right)^{\frac{n}{k-1}} \left( \frac{2k}{k+1} M_m^2 - \frac{k-1}{k+1} \right)^{\frac{1}{k-1}}, \quad M_m = M(x_m). \quad (1)$$

TABLE 1. Range of Experimental Investigations

No.	$M_\infty$	$M_a$	$k$	$D$	$n_\infty$	Body	Lit. source
1		5,0		1,2	2,8-6,3	A $\theta_a = 10^\circ$	[1]
2		4,85		1,6	4,04		
3		«		2,0	3,52-6,34		
4		4,0		2,4	6,38-6,78		
5	7,1	5,3	1,4	1,82	3,4-4,27		
6		«		2,18	4,27		
7		1,0		5,0	1090; 1796		
8		«		6,0	476-3000		
9		«		10,0	1120-1290		
10		«		12,0	1410		
11				7,6	2-23,5	C	[2]
12	2,5	1,0	1,4	16,3	3,18-12,4		
13				33,3	6,3-9,5		
14	3,5		1,4	13,33	55; 142	C	[3]
15	«	«	«	8,0	55; 110		
16	«	«	«	5,0	137	A	
17	«	«	«	13,33	118	C	
18	4,2	1,0	«	«	53; 132	C	
19	«	«	«	8,0	40; 132	C	
20	«		1,67	13,33	121	B	
21	2,5		1,4	«	24; 89,5	A	[4]
22	3,5		«	«	22,1-55		
23	2,5	1,0	1,096	1,2	260	A	
24	1,83	1,0			5,66-49,8	A	Authors' expt.
25	«	2,0			1,36-18,7		
26	«	3,0			1,35-4,8		
27	3,0	1,0	1,4	1,428	24-90	A $\theta_a = 5^\circ$	
28	«	2,0			5,55-27		
29	«	3,0			2,7-7,0		



Note. 1-29 correspond to points of Fig. 2

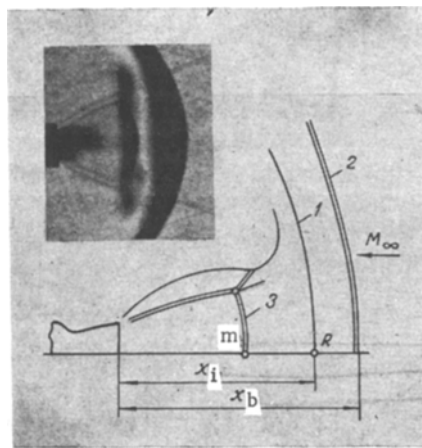


Fig. 1. Qualitative flow pattern in the interaction of an underexpanded jet with an opposing supersonic stream.

Here the pressure  $p_{S\infty}$  is determined from the Rayleigh equation with known  $p_\infty$ ,  $M_\infty$ , and  $k_\infty$ . The dependence  $M(x)$  for jets with different parameters is given in [8], for example.

The values of  $x_m$ , as well as the quantities  $x_i$  and  $x_b$  measured from photographs, were normalized to the corresponding values of  $N$  calculated both with an expansion ratio  $n_\infty = p_a/p_\infty$  and at an expansion ratio  $n_c = p_a/p_c$ . The quantity  $n_c$  was determined from the measured pressure  $p_c$  near the exit cross section of the nozzle under the assumption that the flow in the circulation zone formed ahead of the body is isobaric.

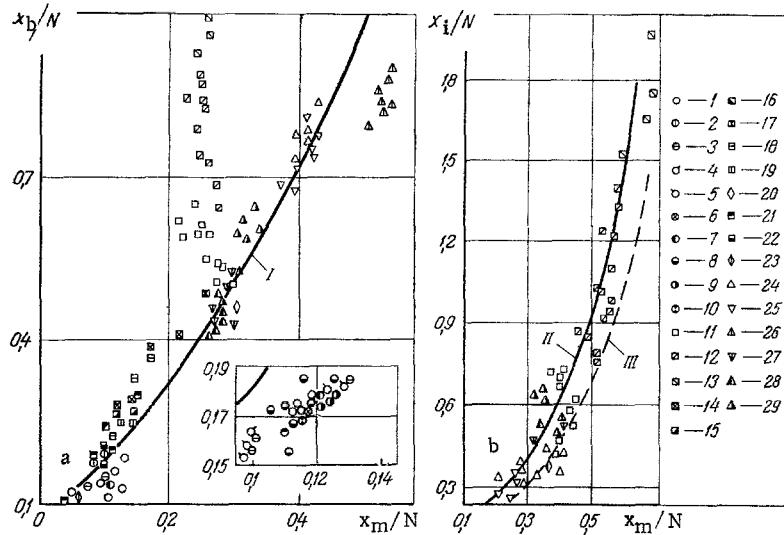


Fig. 2. Dependence of location of bow shock wave (a) and interface (b) on parameters in the jet and the opposing stream: a)  $N = N_\infty$ ; b)  $N = N_c$ ; I) from Eq. (2); II) (3); III) (6).

There are such data in [2] in addition to the experiments of the authors of the article.

The experimental results on the position of the bow shock wave in the stream, treated in the form  $x_b/N_\infty = f(x_m/N_\infty)$ , are presented in Fig. 2a. For  $x_m/N_\infty < 0.3$  all the points are grouped near a single dependence, while for  $x_m/N_\infty > 0.3$  one observes separation of the experimental results into layers with respect to  $D$ . Such modes correspond to large values of  $D$  or, conversely, to small  $P$ . The results of [2] show that in this case the pressure  $p_c$  in the circulation zone differs from  $p_\infty$ , and at the same time, the wave structure of the jet is evidently determined by the pressure  $p_c$ . Treatment of the experimental data on the location of the interface in the form  $x_i/N_\infty = f(x_m/N_\infty)$  gives results qualitatively identical to those given in Fig. 2a: At  $x_m/N_\infty > 0.3$  the data of [2] corresponding to large  $D$  fall out of the general group.

The introduction of the pressure  $p_c$  into the complex  $N$  allows one to liquidate the separation of the experimental results into layers with respect to  $D$ . This is seen, for example, in Fig. 2b, where test data characterizing the location of the interface between the jet and the stream, treated in the form  $x_i/N_c = f(x_m/N_c)$ ,  $N_c = M_a \sqrt{kn_c}$ , are presented.

By analogy with [7], to represent the experimental results in the form of empirical equations we chose the functional dependence

$$\frac{x_m}{N} = 0.745 - A \exp\left(-B \frac{l}{N}\right);$$

$$l = \begin{cases} x_b \\ x_i \end{cases}$$

The coefficients of this dependence were calculated from the experimental data (Table 1) by the least-squares method. In the treatment of the results using the complex  $N_\infty$ , the experimental data of [2] for  $D = 16.3$  and  $33.3$  were not taken into the calculation. The empirical equations obtained, solved for  $x_b$  and  $x_i$ , have the following form:

a)  $x_m/N_\infty < 0.3$ ;  $N = N_\infty$

$$x_b/N = 0.857 G - 0.197; \quad \sigma = 0.035; \quad (2)$$

$$x_i/N = 0.621 G - 0.143; \quad \sigma = 0.049; \quad (3)$$

b)  $x_m/N_\infty > 0.3$ ;  $N = N_c$

$$x_b/N = 1.03 G - 0.292; \quad \sigma = 0.025; \quad (4)$$

$$x_i/N = 0.773 G - 0.206; \quad \sigma = 0.026, \quad (5)$$

where  $G = -\ln(0.745 - x_m/\sqrt{N})$ ; the value of  $x_m$  is calculated from (1);  $\sigma$  is the standard deviation of the points from the corresponding approximating dependence.

Equations (2)-(5) are valid in the following range of parameters:  $M_\infty = 1.83-7.1$ ;  $M_a = 1-5.3$ ;  $k = 1.097, 1.4, 1.67$ ;  $D = 1.2-33.3$ . We note that the parameters of the oncoming stream, which are taken into account through  $p_{s\infty}$  in the calculation of  $x_m$ , do not enter explicitly into these equations.

As shown in [2], the pressure in the circulation zone depends on the form of the front surface of the body from which the jet discharges, the parameters at the nozzle cut and in the oncoming stream, and the value of  $D$ . The analysis made of the experimental results indicates that with an increase in  $P$  or a decrease in  $D$  the characteristic dimensions of the wave structure cease to depend on the concrete dimensions and shape of the body. This evidently indicates that  $p_c$  approaches  $p_\infty$  with an increase in  $P$  (a decrease in  $D$ ).

In Fig. 2b curve III characterizes the dependence of the location of the middle shock in a jet discharging onto an infinite plane barrier on the parameters of the interaction [7]:

$$x_m/N = 0.745 - 0.832 \exp(-1.73 h/N); \quad n = p_a/p_o \quad (6)$$

A comparison of Eqs. (3), (5), and (6) shows that at small values of the argument the calculations by them lead to very close results; with an increase in  $x_m/\sqrt{N}$  a calculation by Eq. (5) gives results higher than those from (3) and (6), although the latter remain close to each other. This indicates the influence of the curvature of the barrier on the location of the middle shock: In the case of strongly concave barriers the central shock is located closer to the nozzle than that ahead of barriers approaching flat ones.

Thus, the choice of the distance to the middle shock as the characteristic dimension and of the pressure  $p_c$  in the circulation zone as the characteristic pressure allows one to use the complex  $N$  as the self-similarity parameter for the longitudinal dimensions of the wave structure of a jet discharging into an opposing stream. As is known, this complex is the self-similarity parameter for free supersonic jets in the gasdynamic [8, 9], transitional, and main sections [10], as well as for jets interacting with infinite plane barriers [7] and for opposing coaxial underexpanded jets [11]. All this, in conjunction with the results presented above, allows one to consider the complex  $N$  as the universal parameter of self-similarity for the longitudinal dimensions of a supersonic underexpanded jet.

In conclusion, the authors express their appreciation to M. I. Vozlinskii for making possible a detailed acquaintance with the experimental results which he obtained.

#### NOTATION

$M$	is the Mach number;
$p$	is the pressure;
$k$	is the adiabatic index of gas jet;
$n$	is the expansion ratio of discharge of jet;
$d$	is the diameter;
$h$	is the distance from nozzle to an infinite plane barrier perpendicular to the jet axis;
$x_m, x_i, x_b$	are the distances from nozzle to middle shock of jet, interface, and bow shock wave, respectively.

#### Indices

$a$	is the parameters of nozzle cut;
$m$	is the middle of body;
$\infty$	is the oncoming stream;
$o$	is the isentropically stagnated stream;
$s$	is the stagnation behind the direct shock;
$c$	is the circulation zone.

The linear dimensions are normalized to the nozzle diameter.

#### LITERATURE CITED

1. D. Faulmann, Etude de l'Interaction de Jets Supersoniques, Ph.D. Thes., Sorbonne (1963).
2. P. J. Finley, J. Fluid Mech., 26, No. 2 (1966).

3. M. I. Vozlinskii, in: *Summaries of Reports of Third All-Union Scientific-Technical Conference on Applied Aerodynamics* [in Russian], Naukova Dumka, Kiev (1973).
4. G. A. Watts, Univ. Toronto IA TN, No. 7, Toronto (1956).
5. R. Cassanova and Lin Wu Yong-Chu, *Phys. Fluids*, 12, No. 12 (1969).
6. V. A. Sukhnev, *Izv. Akad. Nauk SSSR, Mekh. Zhidk. Gaza*, No. 6 (1973).
7. B. G. Semiletenko and V. N. Uskov, *Inzh.-Fiz. Zh.*, 23, No. 3 (1972).
8. G. I. Averenkov, É. A. Ashratov, et al., *Supersonic Jets of Ideal Gas* [in Russian], Vol. 1, Izd. Vychis. Tsent. Mosk. Gos. Univ., Moscow (1970).
9. C. H. Lewis and D. J. Carlson, *AIAA J.*, 2, No. 4 (1964).
10. G. F. Glotov and M. P. Feiman, *Uch. Zap. Tsent. Aero-Gidrodin. Inst.*, 2, No. 4 (1971).
11. E. I. Sokolov and V. N. Uskov, *Inzh.-Fiz. Zh.*, 24, No. 3 (1974).

## GENERALIZATION OF THE CLASSICAL RAYLEIGH EQUATION TO SEVERAL NON-NEWTONIAN LIQUIDS

V. S. Novikov

UDC 532.528:532.529.6

Equations are derived that describe the change in the radius of a spherical gas inclusion in the Bingham, Ellis, Reiner-Rivlin, Shul'man, Kapur-Gupta, and Oswald de Vielle non-Newtonian liquids, as well as in a power-law liquid.

The Rayleigh equation for highly viscous liquids with a finite relaxation time of elastic strains was obtained in [1]. In the present paper this equation is extended to non-Newtonian liquids, for which the rheological equations of state known to the present author are being extended.

In a spherical coordinate system the equation of motion, including strain and the continuity equation, are

$$\rho \left( \frac{\partial v_r}{\partial t} + v_r \frac{\partial v_r}{\partial r} \right) = - \frac{\partial P}{\partial r} + \frac{\partial \tau_{rr}}{\partial r} + \frac{2}{r} \tau_{rr}, \quad (1)$$

$$\frac{1}{r^2} \frac{d}{dr} (r^2 v_r) = 0, \quad (2)$$

if the bubble center is considered to be testing in the liquid. Integrating (2) with respect to  $r$  from the bubble radius  $R$  to infinity, we obtain the radial velocity of motion of the liquid  $v_r = \dot{R} (R/r)^2$ , expressed in terms of the drift velocity of the surface  $\dot{R}$ . Here and elsewhere, the dot over  $R$  denotes differentiation with respect to time. Substituting  $v_r$  into Eq. (1) and integrating it with respect to  $r$  in the limits  $R \rightarrow \infty$ , we obtain

$$\rho (R\ddot{R} + \frac{3}{2} \dot{R}^2) = P_R - P_\infty + \tau_{rr}|_{r=\infty} - \tau_{rr}|_{r=R} + 2 \int_R^\infty \frac{\tau_{rr}}{r} dr, \quad (3)$$

where  $P_R$  and  $P_\infty$  are the pressures in the liquid on the bubble surface and at infinity, and  $\rho$  is the liquid density. As  $P_\infty$  one can take the external static pressure in the liquid. The relation between  $P_R$  and the static pressure in the bubble  $P_0$  is established by the Thomson relation

$$P_R = P_0 - \frac{2\sigma}{R} - \frac{4}{3} \mu_0 \left( \frac{\partial v_r}{\partial r} - \frac{v_r}{r} \right) \Big|_{r=R}, \quad (4)$$

where  $\sigma$  is the surface tension of the liquid. As  $\mu_0$  for non-Newtonian liquids, one can take the slope of the stream curve for small shear stresses (see [2]). The relation between the components of the strain tensor  $\tau_{ij}$  and the components of the velocity deformation tensor  $\dot{\epsilon}_{ij}$ ; i.e., the rheological equation of state, depends on the type of specific non-Newtonian liquid.

---

Institute of Technical Thermal Physics, Academy of Sciences of the Ukrainian SSR, Kiev. Translated from *Inzhenerno-Fizicheskiy Zhurnal*, Vol. 35, No. 4, pp. 677-680, October, 1978. Original article submitted December 5, 1977.